Published in IET Signal Processing
Received on 31st May 2012
Revised on 27th November 2012
Accepted on 22nd January 2013
doi: 10.1049/iet-spr.2012.0161

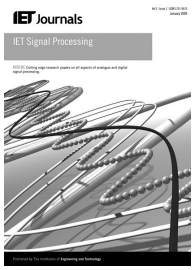

ISSN 1751-9675

Prediction filter design for active noise cancellation headphones

Markus Guldenschuh, Robert Höldrich

Institute of Electronic Music and Acoustics, University of Music and Performing Arts Graz, Inffeldgasse 10, 8010 Graz, Austria
E-mail: guldenschuh@iem.at

Abstract: Digital active noise control (ANC) for headphones usually has to predict the noise because of the latency of common audio converters. In adaptive feedback ANC, the prediction is based on the noise that entered the headphone. This noise is low-pass filtered because of the physical barrier of the ear cups. In this study, this low-pass characteristic is exploited to define a prediction filter which does not require real-time updates. For broadband noises, the prediction filter performs better than adaptive prediction methods like the least mean squares algorithm or iterated one-step predictions in the relevant frequency band. This is shown in simulations as well as in measurements. In addition, the authors show that their prediction filter is more robust against changes in the acoustics of the headphone.

1 Introduction

Active noise control (ANC) systems sense, process and play-back noise such that it interferes destructively with the ambient noise. In headphones, ANC is a very efficient and powerful protection against loud sound levels. It cancels ambient noises directly at the user's ear and reduces the need for loud music play-back.

There are analogue and digital realisations of ANC headphones, whereas digital systems allow more freedom in the controller design. However, the latency of conventional audio converters severely limits the ANC performance [1]. In these cases, the adaptive filter has to predict the noise to compensate for the delay. In the feedback ANC approach, the prediction is based on noise that actually entered the headphone. This has two advantages. Firstly, ANC is independent from the direction of incident noise and also works in diffuse sound fields [2, 3]. Secondly, the upper frequencies of the entered noise are damped by the ear cup. This low-pass characteristic is advantageous when it comes to signal prediction [4].

In literature, prediction is mostly done by different kinds of the least mean squares (LMSs) algorithm [5–7] or by iterated one-step-ahead predictions [8]. Both algorithms are based on sequential updates of the prediction filter and account for changes in the noise-signal characteristics. However, since most environmental noises such as traffic noises are broadband, the signal characteristic of the penetrating noise mainly depends on the assumed constant damping of the ear cups.

In this paper, we therefore suggest the design of a prediction filter that is only based on this passive damping characteristic. The proposed filter does not require run-time coefficient updates, which makes its application simple and economical, and still it yields better and more robust ANC results than the adaptive methods.

The structure of digital feedback ANC is reviewed in the following section and the prediction filter design is outlined in Section 3 and 4. Section 5 shows simulation and measurement results and compares the proposed prediction with LMS and iterated one-step-ahead predictions before the conclusion and an outlook is given in the last section.

2 Digital feedback ANC

Headphones with feedback ANC, as depicted in Fig. 1, only require one microphone inside each ear cup. This microphone measures the residual error signal $e(t)$, which is the superposition of the entered noise $x(t)$ and the played-back anti-noise $y(t)$.

With the analogue/digital converters (ADC and DAC) and the group delay of the secondary path $S(s)$ (i.e. the transfer function from the loudspeaker to the error microphone), there is a delay in the feedback loop; a delay which considerably limits the bandwidth of the ANC. To increase the bandwidth, this delay has to be compensated by predicting future samples of x.

Since x is not directly available, an estimate $\hat{x}$ is obtained by subtracting an estimate $\hat{y}$ of the played-back anti-noise from the sensed residual error, $\hat{x} = e - \hat{y}$. The estimate $\hat{y}$ itself is obtained by feeding the output of the prediction unit through a model $\hat{S}(z)$ of the secondary path and delaying the signal according to the latency of the converters. Owing to the internally generated disturbance signal $\hat{x}$, this feedback controller is called an internal model controller (IMC). For a detailed description of IMCs, we refer to [9].

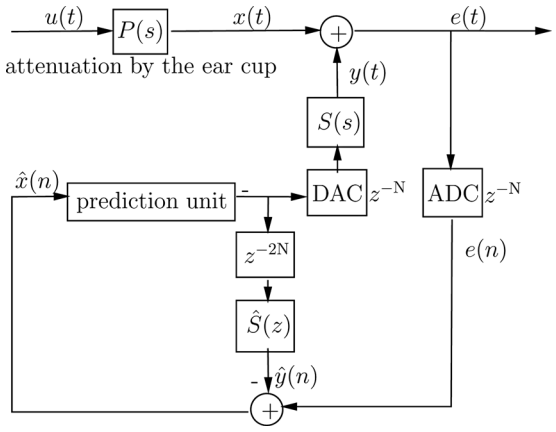

Fig. 1 *Digital feedback ANC:*

An estimate of the noise inside the ear cup $\hat{x}(n)$ is used as input for the prediction unit. The inverted output is played back to cancel the entered noise $x(t)$

3 Noise signal prediction

Assuming that a correct estimate of x is given, $\hat{x}(n)$ equals $x(n-N)$ with N being the delay of one converter in samples. With this, the prediction unit builds a weighted sum of the available past samples to predict the future noise sample

$$x(n+N) = \sum_{i=0}^{L-1} w_i x(n-N-i) \tag{1}$$

with L being the prediction order and w_i the coefficients of a linear prediction filter. The residual error e follows as

$$e(n) = x(n) - \boldsymbol{w}^{\mathrm{T}} \boldsymbol{S} \boldsymbol{x}(n-D) \tag{2}$$

where $\boldsymbol{w}$ is the vector of filter coefficients, $\boldsymbol{S}$ is a convolution matrix of the secondary-path impulse response and $\boldsymbol{x}$ is a signal vector starting from $D = 2N$ samples in the past. The minimum of the expected squared error leads to the well-known Wiener filter [10] and the optimal prediction solution

$$\boldsymbol{w}_{\mathrm{opt}} = \left(\boldsymbol{S}\boldsymbol{R}_x\boldsymbol{S}^{\mathrm{T}}\right)^{-1}\boldsymbol{S}\boldsymbol{r} \tag{3}$$

where $\boldsymbol{R}_x$ is the autocorrelation matrix of the latest available noise samples

$$\boldsymbol{R}_x = \begin{bmatrix} r_0 & r_1 & & r_{L-1} \\ r_1 & r_0 & & r_{L-2} \\ \vdots & \vdots & \ddots & \vdots \\ r_{L-1} & r_{L-2} & & r_0 \end{bmatrix}$$

and $\boldsymbol{r}$ is a vector of autocorrelation elements starting from lag D

$$\boldsymbol{r} = \begin{bmatrix} r_D \\ r_{D+1} \\ \vdots \\ r_{D+L-1} \end{bmatrix}$$

The matrix inversion in (3) can be avoided with the Levinson–Durbin algorithm [11], but only if $D = 1$. The resulting one-step-ahead predictor can still be used for a delay of $2N$ samples when the linear prediction of (1) is iterated $2N$ times. However, since the prediction filter is stable, the recursive one-step-ahead prediction converges to zero. Thus, the filter outputs have to be amplified to get a reasonable multi-sample prediction.

To avoid this problem, gradient search algorithms are often used for prediction problems with more than one sample delay. Gradient search algorithms like the normalised filtered x LMS (FXLMS) use the noise estimate and the error signal to recursively calculate the prediction filter

$$\boldsymbol{w}(n+1) = \boldsymbol{w}(n) + \mu \frac{e(n)\hat{\boldsymbol{S}}\hat{\boldsymbol{x}}}{\hat{\boldsymbol{x}}^{\mathrm{T}}\hat{\boldsymbol{x}}} \tag{4}$$

where μ is the step size parameter which determines the speed of convergence [12, 13]. A large step size leads to a faster convergence, however, with the cost of a slightly larger excess error [10]. Still, in ANC applications a fast adaptation is desired, but the step size has to be bounded by $\mu < (2/\lambda_{\max})$, where $\lambda_{\max}$ is the largest eigenvalue of $\boldsymbol{R}_x$ in order to keep the algorithm stable.

However, the steady update of the coefficients is unnecessary if the main noise characteristic always stays the same. In our ANC application, this is the case because the upper frequencies of the outside noise u (as in Fig. 1) will always be damped by the physical barrier $P(s)$ of the ear cup. This passive attenuation can be written down as a convolution operation

$$\boldsymbol{x} = \boldsymbol{P}\boldsymbol{u}$$

where $\boldsymbol{P}$ is a convolution matrix of a low-pass impulse response that simulates the passive attenuation. With this, the autocorrelation matrix $\boldsymbol{R}_x$ follows to

$$\boldsymbol{R}_x = \boldsymbol{P}^{\mathrm{T}}\boldsymbol{R}_u\boldsymbol{P} \tag{5}$$

Assuming that u is white noise, its autocorrelation matrix $\boldsymbol{R}_u$ reduces to an identity matrix and $\boldsymbol{R}_x$ solely depends on $\boldsymbol{P}$. Thus for white noise u, the calculation of the optimal prediction filter (3) simplifies to

$$\boldsymbol{w}_{\mathrm{opt}} = \left(\boldsymbol{S}\boldsymbol{P}^{\mathrm{T}}\boldsymbol{P}\boldsymbol{S}^{\mathrm{T}}\right)^{-1}\boldsymbol{S}\boldsymbol{p} \tag{6}$$

where $\boldsymbol{p}$ is a vector of the low-pass autocorrelation matrix $\boldsymbol{P}^{\mathrm{T}}\boldsymbol{P}$ starting from time lag D.

In Section 5, we will show that this simplified prediction filter also works for non-white noises, especially if the noises are broadband and their spectral characteristic is still shaped by the passive attenuation P.

The big advantage of (6) is that it allows for an a priori filter design where no real-time calculation of the filter coefficients is needed. All required data [$S(\omega)$ and $P(\omega)$] can be measured and designed in advance. Also, we do not need to rely on an autocorrelation matrix $\boldsymbol{R}_u$ which will never be obtained exactly in real-life applications. The prediction filter that follows from this a priori calculation can be used as a fixed prediction filter in the ANC headphone.

doi: 10.1049/iet-spr.2012.0161

4 Filter design for a prototype headphone

4.1 Passive attenuation of the headphone

The proposed non-adaptive prediction filter (6) depends mainly on the passive attenuation of the headphone. The passive attenuation itself, however, slightly depends on the tightness of the wearing situation and the direction of incident noise. We therefore measured the passive attenuation of a prototype headphone on different persons (including a dummy head) and for different directions of incident sound.

Our prototype headphone is equipped with a microphone inside and a microphone outside each ear cup. Although the outside microphones are not necessary for the feedback ANC application, they are very useful for the measurements of the passive attenuation because they can be used as reference microphone for the outside noise. Thus, we evaluated the passive attenuation P as the relation between the sound pressure level (SPL) P_{in} inside the ear cup and the SPL P_{out} outside the ear cup. $P = (P_{\text{in}}/P_{\text{out}})$ as in Fig. 2.

The measurements were carried out on four persons and a dummy head. The four subjects were asked to once put on the headphone tight and another time to put it on leaky. On the dummy head we measured four scenarios:

1. The headphone is tied tightly to the dummy head.
2. The headphone is put normally on the dummy head.
3. A leak of 1 mm diameter and 15 mm length [The inserted leak has an equivalent electrical resistance of ∼11 MΩ and an inductivity of 23–30 kH.] is introduced between the normally sitting headphone and the ear of the dummy head.
4. A second such leak is introduced between the headphone and the dummy ear.

For each of the above scenarios, we measured P for five different directions of incident sound (front, left, right, back and above) with loudspeakers placed ∼1 m around the test subjects as shown in Fig. 3.

The median passive attenuation over all measurements increases approximately with 12 dB per octave above 500 Hz. This corresponds to a simple second-order filter. We thus propose a second-order low pass with 500 Hz cut-off frequency for the design of the prediction filter. Fig. 4 shows the variations of the passive attenuation in third octave band and the second-order filter $P(\mathrm{j}\omega)$, which is proposed for the prediction filter design. After these a priori measurements in laboratory conditions, no further online measurements of P are necessary for the design of the prediction filter. The deviations of the real measured attenuation from this idealised second-order low pass and their influence onto the ANC performance are examined in Section 5.

Fig. 2 *Measurement of the passive attenuation $P = (P_{in}/P_{out})$ in a tight case on the left and a leaky case on the right*

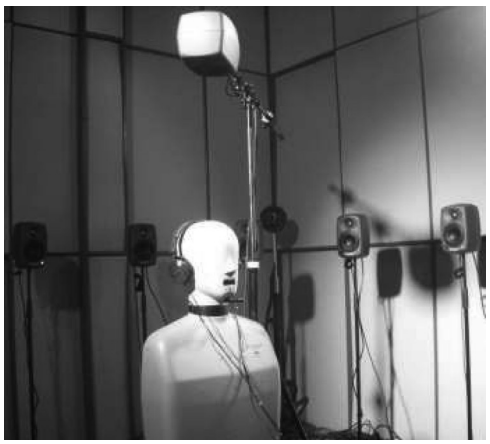

Fig. 3 *Setup to measure the passive attenuation for different directions of incident sound with loudspeakers around and above the test subject*

The passive attenuation was measured for five directions. From 0°, 90°, 180° and 270° in the horizontal plane and from 90° elevation

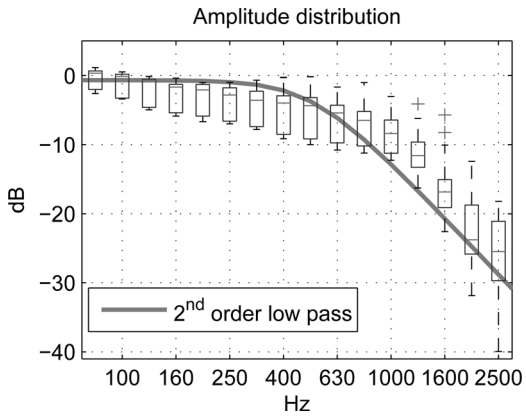

Fig. 4 *Variation of the passive attenuation in third octave bands for different users, different leakage situations and different directions of incident sound*

The boxes include 50% of the measured SPLs and the whiskers show the distribution of all 60 measurements except for the outliers which are marked as crosses. The bars in the middle of the boxes denote the median values of the measured SPLs. The passive attenuation can be approximated by a second-order filter

4.2 Secondary path

The feedback ANC system of Fig. 1 predicts the penetrated noise such that it interferes destructively. However, the anti-noise is played back and modified by the secondary path S (i.e. the loudspeaker) of the headphone. For a perfect noise cancellation, this secondary path would be needed to be compensated. The compensation of S is also indicated in (6) by the pseudoinverse of the convolution matrix $(\boldsymbol{S}\boldsymbol{S}^{\mathrm{T}})^{-1}\boldsymbol{S}$. However, since the loudspeaker response S involves a delay, its inverse is acausal. A perfect compensation of $\boldsymbol{S}$ is thus impossible. Two steps can nevertheless be undertaken to approximately compensate for the secondary path:

1. The group delay of S can be estimated and this group delay can be considered in the prediction filter design as additional time lag $\hat{D}$ for vector $\boldsymbol{p}$ in (6).
2. The amplitude of S can be compensated with a single gain factor $(1/g)$.

The prediction filter is thus calculated as

$$\boldsymbol{w}_{\text{opt}} = \frac{1}{g}\left(\boldsymbol{P}^{\text{T}}\boldsymbol{P}\right)^{-1}\boldsymbol{p} \tag{7}$$

where g is a mean amplitude value of S, and $\boldsymbol{p}$ is a vector of the low-pass autocorrelation matrix $\boldsymbol{P}^{\text{T}}\boldsymbol{P}$ starting from time lag $D + \hat{D}$.

Fig. 5 shows the group delay variation of S for the four test subjects and the dummy head. The group delay is not constant over the frequencies, but the prediction filter design demands one fixed time lag $\hat{D}$. We therefore take the delay of the main pulse in the impulse response of S as fixed time lag. This delay is about 100 µs as can be seen in Fig. 6.

Fig. 7 shows the amplitude variation of the secondary path for the four test subjects and the dummy head in tight and leaky wearing conditions. We propose to take the mean value of the amplitudes between 200 and 600 Hz (i.e. 15 dB) as compensation factor g, because firstly this is the frequency band where we desire good ANC and secondly the amplitudes in this band are very consistent for all test subjects. On the other hand, this means that frequencies below 100 Hz will not always be cancelled in the best possible way since their amplitude is lower than these 15 dB.

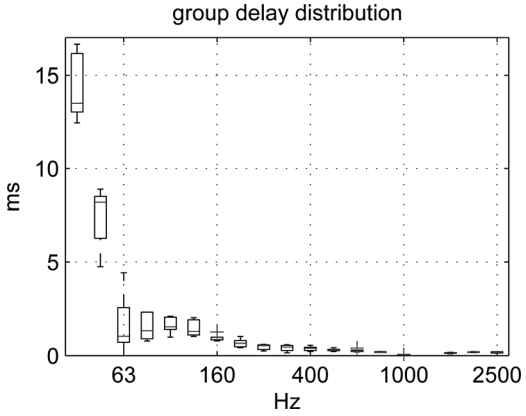

Fig. 5 *Variation of the group delay of S, for four users and a dummy head*

Again, the boxes include 50% of the measured delays and the whiskers show the distribution over all five measurements. The group delay increases largely below 100 Hz

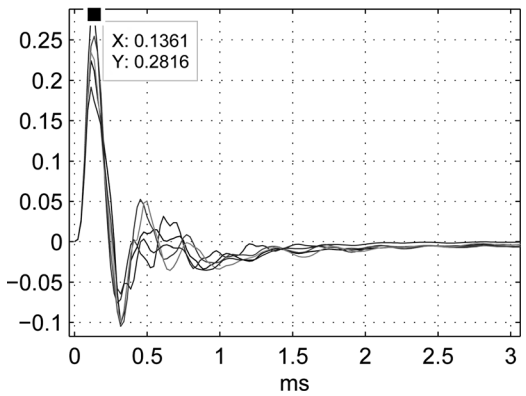

Fig. 6 *Impulse responses of S for four users and a dummy head in tight wearing situations*

The main pulses appear after about 100 µs

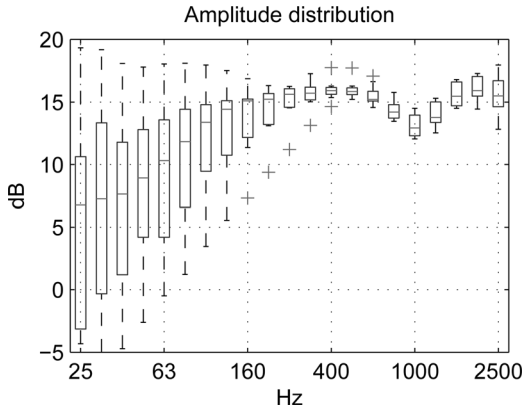

Fig. 7 *Variation of S in third octave bands, for four users and a dummy head*

The amplitudes are roughly constant and do hardly vary above 100 Hz whereas there are large differences between the users and a general high-pass characteristic below 100 Hz

For the prediction filter design, we take the scalar value $g =$ 15 dB that we derived from the laboratory measurements. However, an exact model of S is still required for the IMC in order to get a correct estimate of the penetrated noise $\hat{x}$. Therefore it is crucial for the ANC system that a good model $\hat{S}$ is acquired. While the passive attenuation P was only measured once for all different use cases, the impulse response of $\hat{S}$ has to be measured for every user because it may vary from the laboratory measurement [14].

Since the headphone is used for ANC, the secondary path is usually measured in very noisy conditions. We need at least 10 dB signal-to-noise ratio (SNR) for the measurement because the secondary path S has a dynamic of about 10 dB as can be seen in Fig. 7. Therefore

- we firstly measure a sample of the penetrated noise and apply an A weighting filter to get an estimate of the dBA level.
- Secondly, we use a measurement signal with roughly the same spectral characteristic as the penetrated noise, that is, the second-order low pass from Fig. 4.
- Thirdly, we play back the measurement signal with the dBA level of the noise and increase the SNR to 10 dB by extending or repeating the measurement signal ten times.

$\hat{S}$ is the discrete Fourier transform ($\mathcal{DFT}$) of the measurement response y_S divided by the $\mathcal{DFT}$ of the measurement signal x_S $\left(\hat{S} = \mathcal{DFT}(y_S)/\mathcal{DFT}(x_S)\right)$. In the time domain, it is a deconvolution of y_S with the inverse of x_S.

We propose a sequence of pink noise (which is filtered with the aforementioned second-order low pass) as measurement signal because it is unobtrusive and might even not be noted within the broadband noise from outside. However, any broadband signal like sine sweeps or maximum length sequences will suffice this purpose [15–18]. In any case, the unextended measurement signal needs to be at least 50 ms long in order to be able to measure frequencies down to 20 Hz. With the extension/repetition of the measurement signal the whole procedure lasts a little bit longer than 1 s; after this time, ANC can be started.

In literature, advanced methods for online secondary path identification are proposed [5, 6, 19–22]. These methods are able to track changes in the secondary path during the

doi: 10.1049/iet-spr.2012.0161

active noise cancellation. Such methods are not yet implemented in our ANC system, but since we save resources with our non-adaptive prediction filter, these resources might be used for online secondary path identification. Another strategy is to include an uncertainty model in controller design that allows for some variation in the secondary path as it is done in [23–25]. The consequences of changes in the secondary path onto our ANC system will be examined in the following section.

5 Simulation and measurement results

The following simulations are based on measurement data from our prototype headphone described in the previous section. We have a total latency of $\sim$190 µs, including the loudspeaker response of the headphone and the converter latency. This corresponds to $\hat{D} + D = 8$ samples at 48 kHz sampling frequency. If not indicated differently, we use a 0.2 s long impulse response for S and a 11 ms long version of the same impulse response for $\hat{S}$.

5.1 Investigation on the spectral characteristic of the noise

Now, this eight-sample prediction filter is compared with adaptive methods like LMS and iterated one-step linear prediction. Although the prediction filter is derived under the assumption of white input noise, this comparison is now done for noises with non-white spectral characteristics:

- Static and broadband aeroplane noise.
- Time-varying narrow band noise of an accelerating engine.

The filters have a length of 32 samples in all cases and the step size of the normalised LMS algorithm is set to 0.003 if not indicated differently. This step size is a factor 6 below the maximum stable value for the given inputs and it yields a convergence after < 0.4 s as can be seen in Fig. 8. For the following comparison, only the steady-state error after these 0.4 s is considered.

Fig. 9 shows the spectrum of the aeroplane noise and the spectra of the residual noises after ANC. Our prediction filter yields slightly better results than the iterated one-step prediction filter and – at the same time – consumes far less processing power. The LMS performs slightly better than the two prediction filters between 150 and 300 Hz, and it produces a smaller error above 2000 Hz. However, it therefore only cancels noise up to 600 Hz, which makes it less favourable compared with the fixed prediction filter.

Denote that the LMS filter converges to the H_2 optimal Wiener filter and that the prediction filter can only reach a larger bandwidth, because it allows more error in the upper frequency band. In [23], a constraint on the noise enhancement in the upper frequencies is suggested for ANC in a headrest. In the case of headphones, however, the error in the upper frequency bands has a negligible SPL because of the pronounced passive attenuation.

The excitation noise of the previous simulation was very broadband. Thus the penetrated noise x was above all coloured by the passive attenuation P. We could therefore expect a good result of the proposed prediction filter. In the next simulation, we use the noise of an accelerating engine which is narrow band and time varying. Fig. 10 shows that the LMS algorithm has advantages here, but only if the step size is increased to $\mu = 0.01$. However, this step size is only possible if a good model $\hat{S}$ is implemented. It bears the risk of driving the LMS algorithm unstable for wrong estimates of S as can be seen in the following section. A solution could be an adaptable step size as suggested in [20]. In

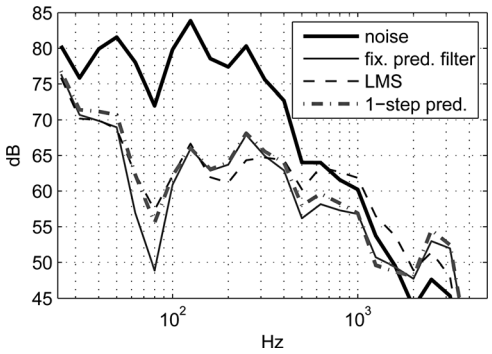

Fig. 9 *Spectrum of the aeroplane noise x that entered the headphone and the residual noises after ANC with the proposed prediction filter, an LMS filter and after iterated one-step-ahead prediction*

The prediction filters yield ANC up to 1.5 kHz, whereas the LMS only cancels noise up to 600 Hz. The deteriorated ANC of all methods below 80 Hz comes because of the long group delay of the loudspeaker in the low-frequency band

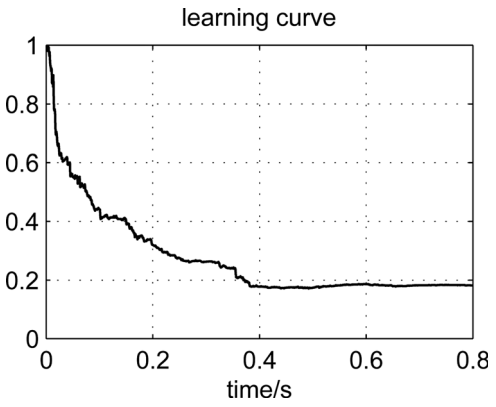

Fig. 8 *Learning curve of the LMS algorithm for the broadband aeroplane noise*

The curve is derived as a cumulative sum of $e^2[n]$ normalised by the cumulative sum of the squared input noise $x^2[n]$

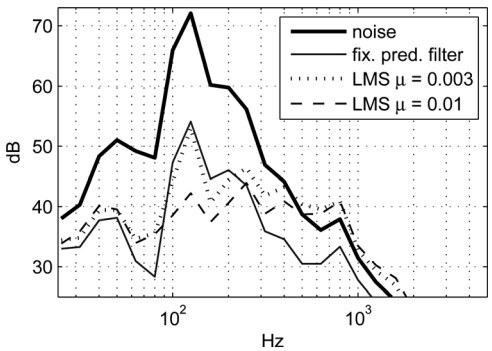

Fig. 10 *Engine noise x that entered the headphone and the residual noises after ANC*

Again, the fixed prediction filter yields ANC in a larger band width than the LMS algorithm. However, if the step size μ is increased to 0.01, the LMS performs better at the spectral peak around 120 Hz

either case, the proposed fix prediction filter yields a much larger ANC bandwidth up to 1.5 kHz again.

5.2 Investigation on variations in the secondary path and the passive attenuation

In the previous simulations, we showed that the proposed prediction filter yields the largest ANC bandwidth independently of the spectral characteristic of the noise. Here, we investigate the influence of variations in S and P on the ANC performance. We investigate the influences of these transfer functions separately although in reality they might be coupled. For example, a leaky wearing situation might deteriorate the passive attenuation and, at the same time, weaken the reproduction of low frequencies in the secondary path.

First, we compare the ANC of the proposed prediction filter for two different passive attenuations. The frequency responses of these attenuations are shown in Fig. 11. The secondary path stays unchanged and the excitation signal is pink noise. Although one measured passive attenuation is much poorer than the other, the difference of the ANC in third octave bands from 20 to 4000 Hz stays below 0.5 dB. Thus the exact knowledge of P is not necessary for the prediction filter design.

Next, we investigate the influence of a wrong secondary-path estimate on the noise prediction. Again, in reality a change in S will not only affect the prediction but the whole feedback ANC system, where a model of S is also needed to estimate the penetrated noise $\hat{x}$. However, we will investigate the influences separately to gain a deeper insight in the ANC system.

Fig. 12 shows the frequency response of the used S and $\hat{S}$. Although $\hat{S}$ has a very flat frequency response, S has a strong drop off below 200 Hz. On the one hand, this means that the given gain correction ($1/g$) will not hold for those frequencies, and we have to expect a poor performance in the low frequencies. On the other hand our prediction filter does not depend on the exact frequency response of S and is thus robust against changes. The FXLMS algorithm however needs a good estimate $\hat{S}$ for its coefficient update as indicated in (4). Fig. 13 shows that the FXLMS with a step size of $\mu = 0.003$ starts to become unstable after 1 s, whereas the fixed prediction filter still yields an ANC of >10 dB between 100 and 200 Hz.

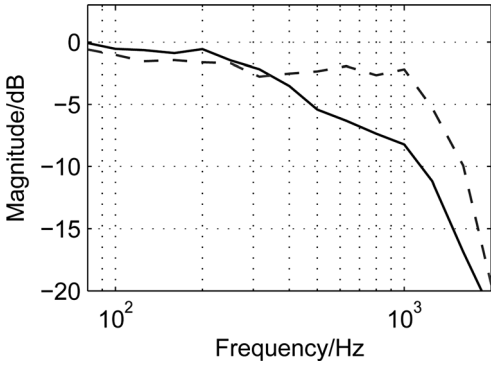

Fig. 11 *Two different frequency responses of the passive attenuation*

The solid one was measured under tight wearing conditions. Therefore the passive attenuation already starts at 400 Hz. The dashed frequency response does hardly attenuate up to 1 kHz. It was measured under a leaky condition

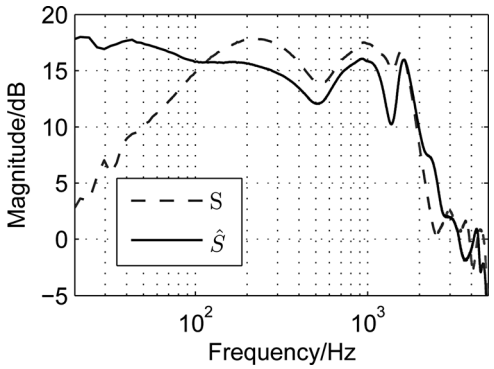

Fig. 12 *Real and estimated secondary path*

They differ considerably, especially below 200 Hz

Finally, we consider the full consequences when S and P change after the initial identification process. Thus, in this simulation also the estimation of $\hat{x}$ via the feedback branch through $\hat{S}$ is affected. The feedback ANC system with the FXLMS algorithm runs unstable before 1 s.

With the transfer functions from Fig. 12, the ANC system with the proposed prediction filter is still stable, but it produces an error of >10 dB around 80 Hz as can be seen in Fig. 14. In general, it has to be said that – without

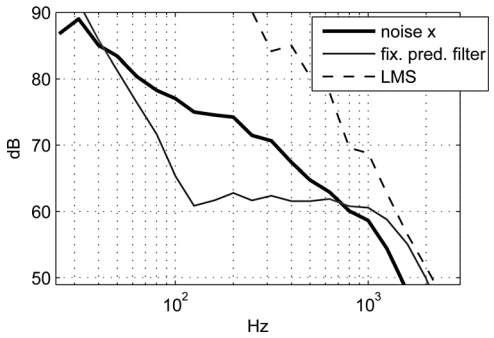

Fig. 13 *Pink noise x and the residual noises after ANC with a wrong estimate of S in the prediction unit*

The FXLMS algorithm which depends on a good model of S starts to become unstable after the simulation time of 1 s. The proposed prediction filter still yields a good ANC performance

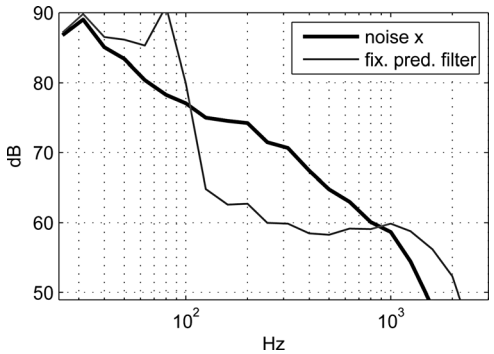

Fig. 14 *Pink noise x and the residual noises after ANC with a wrong estimate of S also in the feedback branch $\hat{S}$ which estimates $\hat{x}$*

While the FXLMS runs unstable within 1 s. The proposed prediction filter still yields good results above 100 Hz, but increases the error considerably below 100 Hz

doi: 10.1049/iet-spr.2012.0161

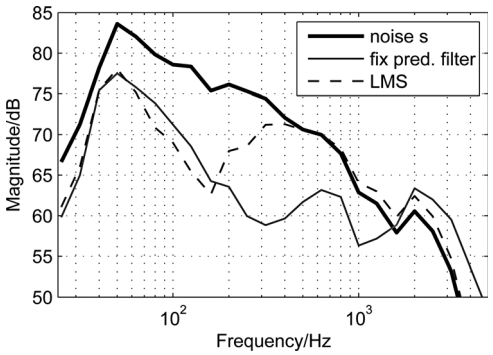

Fig. 15 *Measurement results from pink noise x and the residual noises after ANC*

The proposed prediction filter yields a much better ANC than the FXLMS algorithm between 200 and 1500 Hz with the cost of producing more error above 1500 Hz. Below 50 Hz, the loudspeakers do not produce enough SPL and additionally, the large group delay of S in these frequencies disables a better ANC

further constraints – stability cannot be guaranteed for all deviations from the initially measured secondary path. A robust IMC design that accounts for uncertainties in the secondary path model can be found in [23, 24].

5.3 Measurement result

Finally, we implemented the feedback ANC system on a digital signal processor in order to compare the proposed prediction filter with the LMS algorithm under real conditions. In the implementation, we use a 6 ms impulse response of $\hat{S}$ instead of the 11 ms impulse response. The shorter impulse response saves computational power, especially for the FXLMS which needs two convolutions with $\hat{S}$: one for the update of its coefficients and a second one to obtain the estimate $\hat{x}$ of the penetrated noise (which is generally needed in the digital feedback ANC approach).

The measurement setup equals the one in Fig. 3. As excitation signal, we used pink noise. Fig. 15 shows the results of the measurement. The proposed prediction filter yields an ANC up to over 1000 Hz whereas the FXLMS algorithm only cancels noise up to 400 Hz. As already shown in the simulations, the FXLMS algorithm is much more sensitive to uncertainties in the secondary-path estimate. Also, the adaptive algorithms are more sensitive to sensor noise, which is why the use of a Kalman filter is proposed in [8]. Our prediction filter is very robust against sensor noise and inexact estimates of S and, at the same time, much more economical and efficient than the adaptive methods. It only produces a larger error in the high-frequency band, which can be accepted since the passive attenuation at these frequencies is already very good.

6 Conclusion and outlook

This paper presents a new predictive solution for the biggest problem in digital feedback ANC headphones: The unavoidable delay of the secondary path and the AD/DA conversion. We show that a main part of the noise characteristic is determined by the passive attenuation because of the ear cups. With this information, we design an a priori prediction filter that does not need any real-time coefficient updates and is therefore very economical. To the knowledge of the authors, this elegant prediction solution, elaborated by Jain and Ranganath [4], has never been suggested for feedback ANC applications. Simulations show that this filter reaches equal – if not better – results than adaptive prediction methods like the LMS or an iterated one-step-ahead linear prediction. At the same time, it is more stable against changes in the acoustics of the headphone. For a prototype system, we could show that the feedback ANC system can be kept very simple without any adaptation, but for a commercial product some kind of online secondary path estimation or stability check will be necessary. The proposed prediction filter might also be used in hybrid ANC systems as proposed in [3, 26, 27], where it is expected to lead to improved ANC results, too.

7 Acknowledgments

This work is supported in part by the K-Project AAP. The project is funded in the context of COMET – Competence Centres for Excellent Technologies by BMVIT, BMWFJ, Styrian Business Promotion Agency (SFG), State of Styria – Government of Styria (‘Abteilung 3: Wissenschaft und Forschung’ as well as ‘Abteilung 14: Wirtschaft und Innovation’). The programme COMET is conducted by FFG.

8 References

1 Snyder, S.D., Hansen, C.H.: ‘The influence of transducer transfer functions and acoustic time delays on the implementation of the lms algorithm in active noise control systems’, *J. Sound Vib.*, 1990, **141**, (3), pp. 409–424
2 Zangi, K.C.: ‘A new two-sensor active noise cancellation algorithm’. 1993 IEEE Int. Conf. Acoustics, Speech, and Signal Processing, 1993 (ICASSP-93), 1993, vol. 2, pp. 351–354
3 Rafaely, B., Jones, M.: ‘Combined feedback-feedforward active noise-reducing headset – the effect of the acoustics on broadband performance’, *J. Acoust. Soc. Am.*, 2002, **112**, pp. 981–989
4 Jain, A., Ranganath, S.: ‘Extrapolation algorithms for discrete signals with application in spectral estimation’, *IEEE Trans. Acoust. Speech Signal Process.*, 1981, **29**, (4), pp. 830–845
5 Kuo, S.M., Mitra, S., Gan, W.S.: ‘Active noise control system for headphone applications’, *IEEE Trans. Control Syst. Technol.*, 2006, **14**, pp. 331–335
6 Gan, W.S., Mitra, S., Kuo, S.M.: ‘Adaptive feedback active noise control headset: implementation, evaluation and its extensions’, *IEEE Trans. Consum. Electron.*, 2005, **51**, (3), pp. 975–982
7 Kannan, G., Milani, A.A., Panahi, I.M.S., Briggs, R.W.: ‘An efficient feedback active noise control algorithm based on reduced-order linear predictive modeling of fMRI acoustic noise’, *IEEE Trans. Biomed. Eng.*, 2011, **58**, (12), pp. 3303–3309
8 Oppenheim, A.V., Weinstein, E., Zangi, K.C., Feder, M., Gauger, D.: ‘Single-sensor active noise cancellation’, *IEEE Trans. Speech Audio Process.*, 1994, **2**, (2), pp. 285–290
9 Morari, M., Zafiriou, E.: ‘Robust process control’ (Prentice-Hall, 1989)
10 Haykin, S.: ‘Adaptive filter theory’ (Prentice-Hall, 2001, 4th edn.)
11 Vaidyanathan, P.P.: ‘The theory of linear prediction’, in: ‘Synthesis lectures on signal processing’ (Morgan & Claypool, 2007)
12 Kuo, S.M., Kuo, S., Morgan, D.R.: ‘Active noise control systems: algorithms and DSP implementations Wiley series in telecommunications and signal processing’ (Wiley, 1996)
13 Nelson, P.A., Elliott, S.J., Williams, J.E.F.: ‘Active control of sound’, *Phys. Today*, 1993, **46**, (1), pp. 75–76. Available at http://link.aip.org/link/?PTO/46/75/2
14 Guldenschuh, M., Sontacchi, A., Perkmann, M., Opitz, M.: ‘Assessment of active noise cancelling headphones’. 2012 IEEE Int. Conf. Consumer Electronics – Berlin (ICCE-Berlin), 2012, pp. 299–303
15 Weinzierl, S., Giese, A., Lindau, A.: ‘Generalized multiple sweep measurement’. Audio Engineering Society Convention 126, 2009. Available at http://www.aes.org/e-lib/browse.cfm?elib=14963
16 Farina, A.: ‘Advancements in impulse response measurements by sine sweeps’. Audio Engineering Society Convention 122, 2007. Availableat http://www.aes.org/e-lib/browse.cfm?elib=14106
17 Rife, D.D., Vanderkooy, J.: ‘Transfer-function measurement using maximum-length sequences’. Audio Engineering Society Convention 83, 1987. Available at http://www.aes.org/e-lib/browse.cfm?elib=4900

18 Xiang, N., Schroeder, M.R.: 'Reciprocal maximum-length sequence pairs for acoustical dual source measurements', *J. Acoust. Soc. Am.*, 2003, **113**, (5), pp. 2754–2761
19 Zhang, M., Lan, H., Ser, W.: 'A robust online secondary path modeling method with auxiliary noise power scheduling strategy and norm constraint manipulation', *IEEE Trans. Speech Audio Process.*, 2003, **11**, (1), pp. 45–53
20 Akhtar, M.T., Abe, M., Kawamata, M.: 'A new variable step size LMS algorithm-based method for improved online secondary path modeling in active noise control systems', *IEEE Trans. Audio, Speech, Lang. Process.*, 2006, **14**, (2), pp. 720–726
21 Liu, J., Xiao, Y., Sun, J., Xu, L.: 'Analysis of online secondary-path modeling with auxiliary noise scaled by residual noise signal', *IEEE Trans. Audio, Speech, Lang. Process.*, 2010, **18**, (8), pp. 1978–1993
22 Gholami-Boroujeny, S., Eshghi, M.: 'Online secondary path modeling in active noise control system using PBS-LMS algorithm'. 2010 IEEE Tenth Int. Conf. Signal Processing (ICSP), 2010, pp. 2600–2603
23 Rafaely, B., Elliott, S.J.: 'H2/H infin; active control of sound in a headrest: design and implementation', *IEEE Trans. Control Syst. Technol.*, 1999, **7**, (1), pp. 79–84
24 Kinney, C.E., Villalta, A., de Callafon, R.A.: 'Active noise control of a cooling fan in a short duct'. Proc. ASME NoiseCon/NCAD, 2008, pp. 1–11
25 Kinney, C.E., de Callafon, R.A.: 'Robust estimation for automatic controller tuning with application to active noise control', in 'Model-based control: bridging rigorous theory and advanced technology' (Springer, USA, 2009), ed. HoF, P.M.J. pp. 107–124
26 Song, Y., Gong, Y., Kuo, S.M.: 'A robust hybrid feedback active noise cancellation headset', *IEEE Trans. Speech Audio Process.*, 2005, **13**, (4), pp. 607–617
27 Schumacher, T., Krüger, H., Jeub, M., Vary, P., Beaugeant, C.: 'Active noise control in headsets: a new approach for broadband feedback ANC'. Proc. IEEE Int. Conf. Acoustics, Speech, and Signal Processing, Prague, Czech Republic, 2011, pp. 5183–5203

doi: 10.1049/iet-spr.2012.0161